N O T I C E

THIS DOCUMENT HAS BEEN REPRODUCED FROM MICROFICHE. ALTHOUGH IT IS RECOGNIZED THAT CERTAIN PORTIONS ARE ILLEGIBLE, IT IS BEING RELEASED IN THE INTEREST OF MAKING AVAILABLE AS MUCH INFORMATION AS POSSIBLE

NASA

Technical Memorandum 81989

(NASA-TM-81989) ON EXTRACTING BRIGHTNESS TEMPERATURE MAPS FROM SCANNING RADIOMETER DATA (NASA) 27 p HC A03/MF A01 CSCL 08B

N80-32838

Unclas

G3/43 34228

On Extracting Brightness Temperature Maps from Scanning Radiometer Data

P. Argentiero and R. Garza-Robles

AUGUST 1980

National Aeronautics and
Space Administration

Goddard Space Flight Center
Greenbelt, Maryland 20771

OCT 1980
RECEIVED
NASA STI FACILITY
ACCESS DEPT.

ON EXTRACTING BRIGHTNESS TEMPERATURE MAPS FROM SCANNING RADIOMETER DATA

P. Argentiero
R. Garza-Robles

August 1980

GODDARD SPACE FLIGHT CENTER
Greenbelt, Maryland 20771

ON EXTRACTING BRIGHTNESS TEMPERATURE MAPS FROM SCANNING RADIOMETER DATA

P. Argentiero
R. Garza-Robles

ABSTRACT

The extraction of brightness temperature maps from scanning radiometer data is described as a typical linear inverse problem. Spatial quantization and parameter estimation is suggested as an advantageous approach to a solution. Since this approach takes into explicit account the multivariate nature of the problem, it permits an accurate determination of the most detailed resolution extractable from the data as well as explicitly defining the possible compromises between accuracy and resolution.

To illustrate the usefulness of the method described in this paper for algorithm design and accuracy prediction, it was applied to the problem of providing brightness temperature maps during the NOSS flight segment. The most detailed possible resolution was determined and a curve which displays the possible compromises between accuracy and resolution was provided.

PRECEDING PAGE BLANK NOT FILMED

ON EXTRACTING BRIGHTNESS TEMPERATURE MAPS FROM SCANNING RADIOMETER DATA

1. Introduction

Antenna temperatures measured by a scanning microwave radiometer can be represented as an integral of the energy radiating from the earth's surface weighted by the antenna sensitivity pattern. In the case of an ideal antenna whose sensitivity pattern is effectively a step function, the antenna temperature and the brightness temperature of the corresponding area on the earth are proportional and the one can be inferred from the other. However, actual gain patterns respond significantly to large areas of the earth's surface. Hence, the extraction of detailed and accurate brightness temperature maps from a set of apparent antenna temperatures requires a so-called antenna pattern correction (APC) algorithm.

Several APC procedures have been described in the literature [1]-[4]. Recently, Stogryn [5] pointed out the similarity of the APC problem to that which arises during atmospheric sounding experiments where temperature profiles are desired. The similarity is that in both cases a continuous function is to be inferred from a finite set of observations and each observation is an integral transform of the function. Stogryn suggests the use of Backus-Gilbert theory [6] to develop accuracy versus resolution curves for any given set of antenna temperature observations.

The development of an APC algorithm can be properly viewed as a linear inverse problem [7]. The characteristic features of this type of problem are that a continuous function f must be determined and that the observations are linear functionals of f. Linear inverse problems are common in Geophysics and investigators in this area have developed numerous approaches to a solution [8]. When geographically localized or in situ observations are available, a spatial quantization and linear parameter estimation approach is often used. This technique has been effective in gravity field determination [9] and magnetic field determination [10]. The purpose of this paper is to show that spatial quantization and linear parameter estimation constitutes a particularly natural and suitable approach to the APC problem which can directly lead to a tractible and accurate algorithm for

extracting a geographically referenced brightness temperature map from a set of antenna temperature observations.

In section 2, the development of an APC algorithm is exhibited as a conventional linear inverse problem. Also, a procedure is given for determining the most spatially detailed characterization of a brightness temperature map which a given set of antenna temperature observations can support. Additionally, this section describes a technique for developing APC algorithms which deliver optimal accuracy for any given resolution level. Section 3 considers some of the computational aspects associated with the APC problem and describes some compromises and approximations which can yield effective and computationally efficient APC algorithms. Also, this section shows how the flexibility of the spatial quantization approach can be used to exploit knowledge of the location of sea-land boundaries in the estimation process. In section 4, the concepts and techniques explained in sections 2 and 3 are used to provide an example of a representative APC algorithm for the Large Antenna Multifrequency Microwave Radiometer (LAMMR) on the National Oceanic Satellite System (NOSS).

2. A Linear Inverse Formulation Of The APC Problem

Consider a radiometer observing the earth from an orbiting satellite. By ignoring the effects of a finite integration time, one can assume that an observation T_A^i of antenna temperature is obtained at an observation time indexed by i. Let S_o^i be the associated boresight unit vector. The observation can be represented as

$$T_A^i = \frac{1}{4\Pi} \int_R G(S_o^i, S) T_B(\rho)\, d\Omega \tag{1}$$

where S is a unit vector from the antenna in the direction of the differential solid angle $d\Omega$. The region of integration R is the solid angle which includes all directions S which intercept the portion of the earth visible from the satellite. In equation 1, $G(S_o^i, S)$ is the *antenna pattern function* which satisfies the normalization condition

$$\int_{4\Pi} G(S_o^i, S)\, d\Omega = 4\Pi \tag{2}$$

The symbol $T_B(\rho)$ represents the brightness temperature at some specified frequency and at a point on the earth's surface identified by a unit vector ρ pointing from the earth's center. Since it is desired to refer measurements to particular areas of the earth, it is convenient to change the variable of integration in equation 1 to a differential surface area dA on the earth. This is accomplished as

$$d\Omega = \frac{(-S \cdot \rho)\, dA}{\ell^2} \tag{3}$$

where ℓ is the distance from the antenna to the differential surface element dA. Hence

$$T_A^i = \frac{1}{4\Pi} \int_E G(S_o^i, S) \frac{(-S \cdot \rho)}{\ell^2} T_B(\rho)\, dA \tag{4}$$

where E is the area on the earth viewed by the satellite. Since the satellite orbit and the time history of the antenna pointing direction in spacecraft coordinates are known, the vectors S_o^i and S as well as the distance ℓ are known functions of ρ. This implies that equation 4 can be simplified to

$$T_A^i = \frac{1}{4\Pi} \int_E g_i(\rho) T_B(\rho)\, dA \tag{5}$$

Equation 5 is valid assuming the data has been corrected for cross polarization effects and that a small contribution due to cosmic background noise has been subtracted from the data. The dependence of the brightness temperature function on viewing angle has also been surpassed.

Assume that N such observations are available and are arranged in a column vector symbolized by $\overline{T}_A$. From knowledge of $\overline{T}_A$, one desires as much information as possible about the brightness temperature function T_B. According to equation 5, each scalar element of $\overline{T}_A$ is related to T_B by means of a linear functional. Hence,

$$\overline{T}_A = L(T_B) \tag{6}$$

where the linear transform $L : H \rightarrow E^N$ is a mapping from the Hilbert space of integrable functions on E to Euclidean N space E^N. The Kernal space $K \subset H$ of L consists of all functions $f \in H$ such that $L(f) = \overline{O}$ where $\overline{O}$ represents the N dimensional null vector. The transform L is one to one if and only if K consists of only the null function $f_0 \in H$. However, one can show that for any finite data set T_A, the Kernal space K is necessarily infinite dimensional [11]. It follows that it is not possible to identify a unique brightness temperature function from a set of antenna temperature observations. This is an exhibition of the so-called "ill-posed" nature [8] of linear inverse problems.

To obtain uniqueness the terms of the problem must be changed. Conventionally this is done by utilizing knowledge of the physical nature of the signal to restrict the class of admissable functions. In most cases this involves the imposition of smoothing assumptions. Specifically, assume that the brightness temperature function to be estimated is included in a subspace $H' \subset H$ of H. It is desirable that the space H' be so chosen that when the transform L is restricted to H', it is invertible. Hence, define $L' : H' \rightarrow E^N$ to be identical to L on H'. The transform L' is one to one and, hence, invertible if and only if

$$H' \cap K = \{f_0\} \tag{7}$$

In words, the restriction of L to L′ is invertible if and only if the intersection of the subspace H' of H with the kernal space K of L is the zero dimensional space consisting only of the null function f_0. The art of solving APC problems in particular and linear inverse problems in general is that of finding the least restrictive and most physically realistic subspace H' of functions which satisfies equation 7.

The smoothing assumption required to define H' can be defined either in the spatial or the frequency domain. In the case of APC algorithm development there are advantages to imposing smoothing assumptions in the spatial domain. Hence, let $\{B_j\}_j$ be a decomposition of E into K regularly shaped, disjoint regions. For instance, each set B_j can be defined is a square area on the earth's surface in a longitude-latitude coordinate set. Alternatively, any one of numerous schemes [12] can be employed to define the sets $\{B_j\}_j$ as equal area rectangles in a longitude-latitude coordinate set. Define H' as follows

$$H' = \left\{ T_B \;\middle|\; T_B = \sum_{j=1}^{K} \chi_j T_B^j \right\} \tag{8}$$

where χ_j is the characteristic function of B_j. If $T_B \in H'$, then T_B^j represents the constant value that T_B assumes on the set A_j. It follows that T_B is completely characterized by a K dimensional column vector $\{T_B^j\}_j$ and the problem of estimating T_B from a set of antenna measurements reduces to the problem of estimating a finite set of parameters. In what follows, assume that E has been divided into a finite set $\{B_j\}_j$ of areas and that the brightness temperature to be estimated is included in the function subspace H' as defined in equation 8. No confusion should result by now identifying the symbol $T_B \in H'$ which formally represented a brightness temperature function with the set of parameters $\{T_B^j\}_j$ which characterize it.

According to equation 5, equation 6 can now be given the matrix formulation

$$\bar{T}_A = A\, T_B \tag{9}$$

where A represents an N by K matrix and is defined by

$$A(i,j) = \frac{1}{4\Pi} \int_{B_j} g_i(\rho)\, dA \tag{10}$$

The matrix A can be simply interpreted. Let P^i and S^i respectively be the satellite position vector and antenna boresight direction vector at the instant that observation T_A^i is obtained. Then A(i, j) is the integral of the antenna pattern function over the solid angle subtended by area B_j on the earth's surface when the satellite is in position P^i and the antenna boresight is in a direction given by S^i.

At this point it is useful to introduce statistical concepts by recognizing that the actual observation vector $\bar{T}_A'$ which is obtained by the measuring process is the ideal observation vector $\bar{T}_A$, whose components are given by equation 1, plus a contribution due to thermal noise. Hence,

$$\bar{T}_A' = \bar{T}_A + \nu,\ E(\nu) = O,\ E(\nu\nu^T) = Q \tag{11}$$

Let $\hat{T}_B$ be an estimate of T_B obtained as a linear function of $\bar{T}_A$. A conventional statistical measure of the quality of $\hat{T}_B$ as an estimator is given by

$$M(\hat{T}_B) = \text{TRACE}\,[E\,[(\hat{T}_B - T_B)(\hat{T}_B - T_B)^T]] \tag{12}$$

The object is to find a $\hat{T}_B$ as a linear combination of $\bar{T}_A$ which minimizes $M(\hat{T}_B)$. This is generally called the *minimum variance estimate* of T_B. This can also be considered as a *least squares solution* since the estimate which minimizes the right side of equation 12 will also minimize the quadratic form [13]

$$q = (\bar{T}_A' - A\hat{T}_B)^T Q^{-1} (\bar{T}_A' - A\hat{T}_B) \tag{13}$$

The solution is known to be [13]

$$\hat{T}_B = (A^T Q^{-1} A)^{-1} A^T Q^{-1} \bar{T}_A' \tag{14}$$

Generally the thermal noise can be considered as stationary and uncorrelated over the satellite pass and the covariance matrix Q assumes the form

$$Q = \sigma^2 I \tag{15}$$

where I is the N dimensional identity matrix. Assuming the validity of equation 15, the minimum variance or least squares solution can be written as

$$\hat{T}_B = (A^T A)^{-1} A^T \bar{T}_A' \tag{16}$$

The statistical properties of the solution given by equation 16 are

$$E(\hat{T}_B) = T_B \tag{17a}$$

$$E[(\hat{T}_B - E(\hat{T}_B))(\hat{T}_B - E(\hat{T}_B))^T] = \sigma^2 (A^T A)^{-1} \tag{17b}$$

The matrix $A^T A$ to be inverted in equation 16 is non-singular if and only if the choice of H' as defined by equation 8 satisfies equation 7. If this is the case then equation 16 can be interpreted as specifying the unique function T_B in H' which best fits the data according to fitting criterion q as defined in equation 13. In this sense one is provided a technique for extracting the most accurate possible estimate of T_B from the data set $\bar{T}_A'$ at the resolution level defined by the decomposition of E into areas $\{B_j\}_j$. Assume further that $\{B_j\}_j$ represents a decomposition of E into equal area rectangles and let $|B_j|$ represent the common equal area. The maximum resolution which is achievable in the recovery of T_B from a data set $\bar{T}_A'$ can be described as follows: Let B be the set of all equal area decompositions of E for which the associated matrix $A^T A$ is invertible. Then define

$$|B|_{min} = \min\left\{ |B_j| \;\middle|\; \{B_j\}_j \in B \right\} \tag{18}$$

The maximum resolution achievable from a data set $\bar{T}_A'$ is defined to be $|B|_{min}$. A minimum variance or least squares solution for T_B associated with an equal area decomposition of common area $|B|_{min}$ will be referred to as a *maximum resolution solution.* For any given data set a maximum resolution solution can be approximated by forming and inverting the matrix $A^T A$ for increasingly

finer equal area decompositions of E until inversion difficulties are encountered. This ability to determine a maximum resolution solution solution represents an advantage over the Gilbert-Bacus method [5]. The spatial quantization approach as described in this paper takes into explicit account the multivariate nature of the APC problem. Thus, it is capable of determining at what resolution uniqueness is lost by examining the invertibility properties of a well defined set of square matrices. By contrast, the Bacus Gilbert method cannot be conveniently used to determine maximum resolution.

In addition, it follows from equation 17b that one can compute the accuracy with which T_B can be recovered at any given resolution level before the data is actually obtained. Hence, computer simulations based on equations 10 and 17b can be employed to influence design parameters of a mission as well as to develop optimal estimation strategies and predict expected accuracies.

3. Computational Considerations

If N observations are available and K brightness temperature parameters are to be estimated, the least squares algorithm given by equation 16 implies N by K separate evaluations of the right side of equation 10. In most cases this represents a heavy computational burden. Fortunately the localized character of antenna observations permits one to decompose the large dimensional estimation problem defined by equation 16 into several smaller dimensional estimation problems while introducing very little error. Specifically, attention is focused on a single brightness temperature parameter T_B^j associated with a region B_j. Intuitively it is clear that only antenna temperature observations whose associated boresight vectors intersect the earth at points near to the region B_j contain information which is useful in estimating T_B^j. Also the model used in processing this data set to estimate T_B^j need only take into account brightness temperature parameters whose associated regions are within a certain neighborhood of B_j. Define two brightness temperature parameters T_B^i and T_B^j to be *uncoupled in data set* $\bar{T}_A$ if no observation in $\bar{T}_A$ experiences a non-zero contribution from both regions B_i and B_j. Otherwise, brightness temperature values T_B^i and T_B^j are referred to as being *coupled in data set* $\bar{T}_A$. One can show [14] that in processing $\bar{T}_A$ or any subset of $\bar{T}_A$ to obtain a minimum variance estimate of a given parameter T_B^i, it is only necessary to include in the model those parameters which are coupled with T_B^i in the data set. Hence attention is directed to equation 9 which provides the model for the data reduction and concentration on estimating a single brightness temperature parameter as a linear function of surrounding data points. Without loss of generality, assume the parameter to be estimated is the first element T_B' in the parameter list T_B. The vector $\bar{T}_A'$ is the set of N' observations, which are associated with points on the earth which are within a sufficiently small radius of B_1, to contribute to a solution. The $K' + 1$ dimensional parameter vector T_B in equation 9 is completed by including the K' parameters that are coupled with T_B' in the data set. Equation 16 can now be implemented for a reduced dimensional minimum variance solution. Let V be the 1 by N' vector which is the first row of the matrix $(A^T A)^{-1} A^T$ which appears in equation 16. Then

$$\hat{T}_B' = V\bar{T}_A' \tag{19}$$

Equation 19 expresses the minimum variance estimate of T_B' as a normalized linear combination of data points in the vicinity of B_1. The computation of V will depend on the density and distribution of data points about the block B' on which T_B' is defined. For a typical satellite mission this distribution will vary somewhat from block to block and from pass to pass. Hence the sampling coefficients used to determine a parameter estimate cannot be precomputed while strictly preserving optimality. However, if the density and distribution do not vary a great deal one can consider the coefficients of an optimal sampling to be obtained from a fixed sampling function. To be specific, assume that the coefficient associated with each data point in an optimal linear estimate of T_B' is obtained by evaluating a polynomial sampling function $P(\theta - \theta', \lambda - \lambda')$ where θ' and λ' are respectively the latitude and longitude of the midpoint of B_1 and where θ and λ are respectively the latitude and longitude of the data point in question. The sampling polynomial can be determined by computing V of equation 19 for a single cononical data distribution and finding the 2 dimensional polynomial which best fits the optimal sampling coefficients in a least squares sense.

The quantity of data required for an optimal estimate of a given brightness temperature parameter and the coefficients of the optimal sampling polynomial can be computed from knowledge of the geometric distribution of the data set and the antenna pattern function. Hence computer simulations performed before mission implementation can determine for any resolution level an efficient APC algorithm and the expected accuracy associated with the algorithm. A strong advantage of this procedure is that the actual data processing would not involve an execution of the expensive algorithm implied by equation 10.

The reader should also notice the great flexibility provided by the spatial quantization approach to the development of an APC algorithm. The procedure is applicable to any decomposition of the viewing area E into disjoint regions $\{B_j\}_j$. Hence it is straightforward to choose the decomposition $\{B_j\}_j$ to exploit knowledge of the spatial properties of the brightness temperature map T_B. In areas where T_B is expected to change slowly, each region can subtend a large area, and where

significant gradients are expected, each region can be defined to subtend a smaller area. Also, it is advantageous to arrange the regions so that their boundaries are congruent to land-sea boundaries where emissivity differences cause discontinuities in the brightness temperature.

Another feature of the procedure described in this paper is exhibited when multifrequency antenna temperature data sets are available and the antenna pattern functions at the various frequencies are substantially different. It is often required to produce a coregistered multivariate data set consisting of brightness temperature at the various frequencies. This problem can be directly solved by implementing the spatial quantization method to develop the highest resolution brightness temperature map at each frequency. A multivariate and coregistered data base can be developed at a given resolution level by a simple resampling process since each scalar brightness temperature map is geographically referenced.

4. An Example

To provide an example of the application of the spatial quantization approach to estimating brightness temperature functions, attention was focused on the NOSS whose goal is to obtain measurements of ocean surface parameters and to provide processed geographical data to primary users within 80 minutes of data receipt at the processing center. Among the instruments that have been selected for use on the NOSS flight segment is the Large Antenna Multifrequency Microwave Radiometer (LAMMR). The LAMMR will provide pixels at a rate of approximately 256 per second for each of 7 channels and for horizontal and vertical polarizations. The result is that several million pixels are generated for every 100 minute orbit. By far, the most expensive component in the LAMMR data processing operation is the APC algorithm and it is in this area that attention must be focused to obtain acceptible accuracy and efficiency. In what follows the intent is to illustrate the use of the techniques described in this paper for algorithm design and accuracy prediction rather than to provide specific results applicable to the NOSS flight segment.

The LAMMR embodies a 3.6 meter aperture antenna which scans the earth in a circle of 43° half cone angle from nadir. Data sampling occurs during the forward 120° of rotation as shown in Figure 1. The basic specifications and major characteristics of LAMMR as used in the computer simulations are given in Table 1. The half power beam width ranges from seven to forty kilometers and the swath width is about 1300 kilometers. The LAMMR will be flown on board an observatory class satellite in a circular orbit at an altitude of 650-760 km with an inclination between 70° and 110°.

The results which follow were obtained from a FORTRAN program which simulates the recovery of a brightness temperature map from an antenna temperature data set. A 700 km, polar orbit was assumed and for simplicity, the effect of earth rotation was ignored. The program was written so that the antenna pattern function was a separate subroutine and, thus, easily modified. The regions used for the spatial quantization are squares in a longitude, latitude space whose size is specified by the user. The simulations occur near the equator so the regions are of nearly equal

area. The numbers on Table 1 imply a data density shown on Figure 2. The square regions shown on the figure are approximately 20 km by 20 km in size and the points on the figure represent the intersection of the boresight vectors with the earth's surface. Hence, if 20 km resolution is required, the ratio of data points to parameters to be estimated is about 10 to 1. The antenna pattern function was chosen to be a reference pattern for the 4.3 GHz frequency and is shown in Table 2. The format for the simulations can be simply described. A sequence of resolution levels at 5 km increments are successively investigated. At each resolution level a grid of square regions is arranged along the satellite subtrack. Attention is focused on the estimation of a single temperature parameter associated with a region on the satellite subtrack and the covariance matrix of the minimum variance solution as given by equation 17b is computed. To accomplish this it is necessary to determine how many parameters are coupled with the parameter in question so that they can be included in the solution, and how much data should be included in the solution. The number of parameters to be included can be determined by examining the fractional response of an antenna temperature observation to a particular grid of regions. For instance, Figure 3 shows the fractional response of an observation to a grid of regions that are 20 km on a side. The bull's eye shows the approximate location of the boresight vector intersection and the numbers shown were computed assuming the antenna pattern function shown in Table 2. An examination of Figure 3 shows that if two regions are separated by at least two other regions they are virtually decoupled in the data. Hence, to estimate a temperature parameter associated with a 20 km by 20 km region, it is sufficient to include in the solution the temperature parameters associated with the twenty-four nearest regions. It follows that the dimension of the estimation problem whose solution is simulated is reduced to twenty-five. The quantity of data to be included in a solution is determined by a trial and error method. All data within a square area centered on the region in question is included in the solution, the area is incremented by 10 km and the process is repeated. As an example, when the resolution required is between twenty and forty kilometers, data within an area seventy kilometers on a side is sufficient to provide an optimal solution. This implies that an optimal estimate of brightness temperature parameters can be obtained as a linear combination of about ninety antenna temperatures.

To implement equation 17b to obtain the covariance matrix of a minimum variance solution requires the computation of the elements of the matrix A as defined in equation 10. Recall that each element of A is the integral of the antenna pattern function over the solid angle subtended at the satellite by a specified region on the earth. The simulation program computes these elements numerically by uniformly distributing one hundred and twenty one points over a specified region. For a given satellite position and antenna boresight direction the antenna response along the line of sight to each point is computed. The values are averaged and then multiplied by the solid angle subtended at the satellite by the region. Once these elements are formed, obtaining the required covariance matrix is just a matter of performing the matrix operations defined in equation 17b.

The results of the simulations are shown on Figure 4. At a 15 km resolution, matrix inversion difficulties are encountered. This implies that solutions are not unique at resolutions of 15 km and less. As shown on Figure 4, a unique solution is available at a 20 km resolution. These results imply that the optimal resolution extractible from the data is between 15 and 20 km.

Figure 4 displays the standard deviation with which a brightness temperature map can be recovered at 4.3 GHz under the assumptions provided by Table 1 and Figure 2. The results are proportional to the standard deviation of the thermal noise which in this case is taken to be 1° K. The figure explicitly shows the compromise between accuracy and resolution which applies for this particular data reduction problem.

5. Conclusions

The extraction of brightness temperature maps from antenna temperatures is a conventional linear inverse problem. In this context the spatial quantization and parameter estimation approach to a solution is particularly applicable. The flexibility of this approach permits ready incorporation of apriori signal information such as the location of land-sea boundaries. Also, since the multivariate nature of the problem is taken into explicit account, it permits a determination of the most detailed resolution at which a brightness temperature map can be estimated.

It is also possible to exploit the in situ character of antenna temperature observations to estimate local blocks of brightness temperature parameters in local blocks of data. This procedure can represent a substantial reduction in computer time. If the data distribution is dense and fairly uniform a further reduction can be achieved by precomputing a polynomial sampling function.

To illustrate the usefulness of the spatial quantization and parameter estimation approach for algorithm design and accuracy prediction, it was applied to the problem of extracting brightness temperature maps from antenna temperatures during the NOSS flight segment. It was shown that at 4.3 GHz, the finest resolution achievable from the data is between 15 and 20 km. A curve which shows the compromise between accuracy and resolution was also provided.

References

1. Buck, G., and Gustincic, J., "Resolution Limitations of a Finite Aperture" IEEE Trans. Antennas Propagat., Vol. AP-15, PP 376-381, 1967
2. Claassen, J., and Fung, A., "The Recovery of Polarized Apparent Temperature Distribution of Flat Scenes From Antenna Temperature Measurements" IEEE Trans. Antennas Propagat., Vol. AP-22, PP 433-442, 1974
3. Holmes, J., Balanis, C., and Gruman, W., "Application of Fourier Transforms For Microwave Radiometric Inversions" IEEE Trans. Antennas Propagat., Vol. AP-23, PP 797-806, 1975
4. Gruman, W., Balonis, C., and Holmes, J., "Three-dimensional Vector Modeling and Restoration of Flat Finite Wave Tank Radiometric Measurements" IEEE Trans. Antennas Propagat., Vol. AP-25, PP 95-104, 1977
5. Stogryn, A., "Estimates of Brightness Temperatures From Scanning Radiometer Data" IEEE Trans. Antennas Propagat., Vol. AP-26, PP 720-726, 1978
6. Backus, G., and Gilbert, F., "Uniqueness In the Inversion of Inaccurate Gross Earth Data" Phil. Trans. Roy. Soc. London, Vol. A266, PP 123-192, 1970
7. Sabatier, P., "Comparative Evolution of Inverse Problems" NASA Tech. Memo. X-62. 150, 1971
8. Parker, R., "Understanding Inverse Theory" Ann. Rev. Earth-Planet. Sci., PP 35-64, 1977
9. Argentiero, P., and Lowrey, B., "A Comparison of Satellite Systems For Gravity Field Measurement" Geophysical Surveys, 1978
10. Damparey, C., "The Equivalent Source Technique," Geophysics, Vol. 34, No. 1, Feb., 1969
11. Sabatier, P., "Remarks On Approximate Methods In Geophysical Inverse Problems" Proc. R. Soc. London, PP 337-349, 1974
12. Hajela, D., "Equal Area Blocks For The Representation of The Global Mean Gravity Field," Ohio State University Dept. of Geodetic Science Report no. 224, 1977

13. Deutch, R., "Estimation Theory," Prentice-Hall, Inc., 1965

14. Argentiero, P., "A Comparison of Least Squares Collocation With Conventional Least Squares Techniques" Bulletin Geodesique, 51, 1977

Table 1. Significant LAMMR Characteristics

Weight (kgm)	318
Effective Aperture (m)	4.0
Swept Volume in Orbit (m^3)	140
Power (W)	300
Primary Radiometer Frequencies (GHz)	4.3, 5.1, 6.6, 10.65, 18.7, 21.3, 36.5
Primary Radiometer Wavelengths (cm)	0.8, 1.4, 1.6, 2.8, 4.5, 5.8, 6.9
Scan Rate (rps)	1
Swath Width (km) (for 120° Scan)	1300
Beamwidth (°)	0.26 to 1.3
Pixels per Scan	256
Water Temperature Precision (°K)	1
Pointing Knowledge (°)	0.03 (3 σ)

Table 2. Reference Pattern for 4.3 GHz

Angle (degrees)	Gain (dB)	Integrated Power
0.00	44.0	.017
0.10	43.9	.067
0.20	43.7	.147
0.30	43.3	.249
0.40	42.8	.365
0.50	42.1	.486
0.60	41.2	.603
0.70	40.2	.700
0.80	38.9	.799
0.90	37.4	.870
1.00	35.6	.922
1.10	33.4	.956
1.20	30.8	.977
1.30	27.6	.987
1.40	23.4	.988
1.50	17.1	.990
1.60	1.5	.993
1.70	10.0	.993
1.80	15.6	.994
1.90	17.6	.995
2.00	18.0	.997
2.10	17.6	1.0
2.20	15.6	1.0
2.30	10.0	1.0
2.40	1.5	1.0

LIST OF FICURES

Figure 1. LAMMR Scan Parameter Geometry

Figure 2. LAMMR Data Density Superimposed on a 20 km by 20 km Grid

Figure 3. Fractional Response x 10^4 of an Antenna Observation (4.3 GHz) to a 20 km by 20 km Grid

Figure 4. Standard Deviation of the Estimated Brightness Temperature Map as a Function of Resolutions

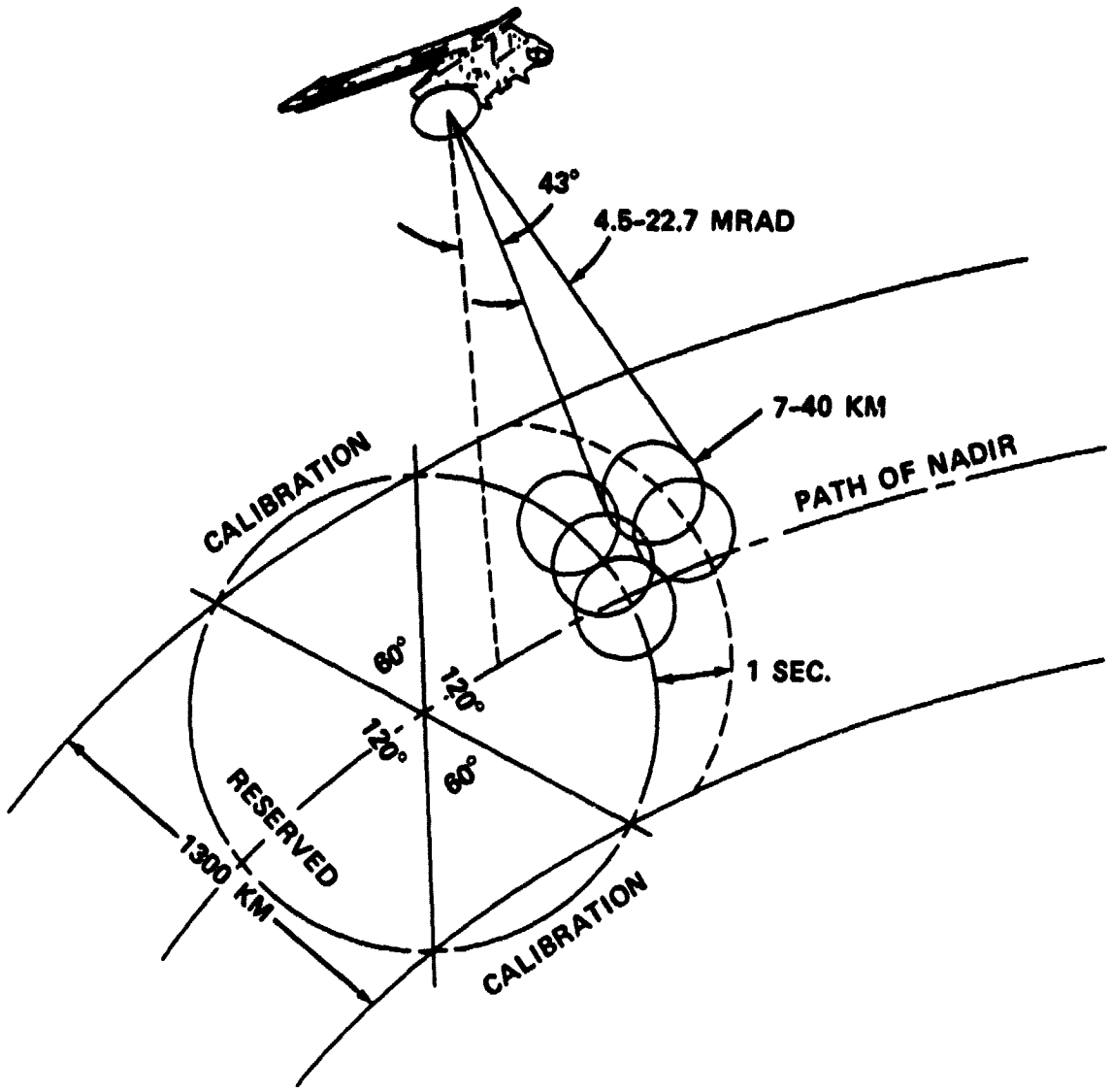

Figure 1. LAMMR Scan Parameter Geometry

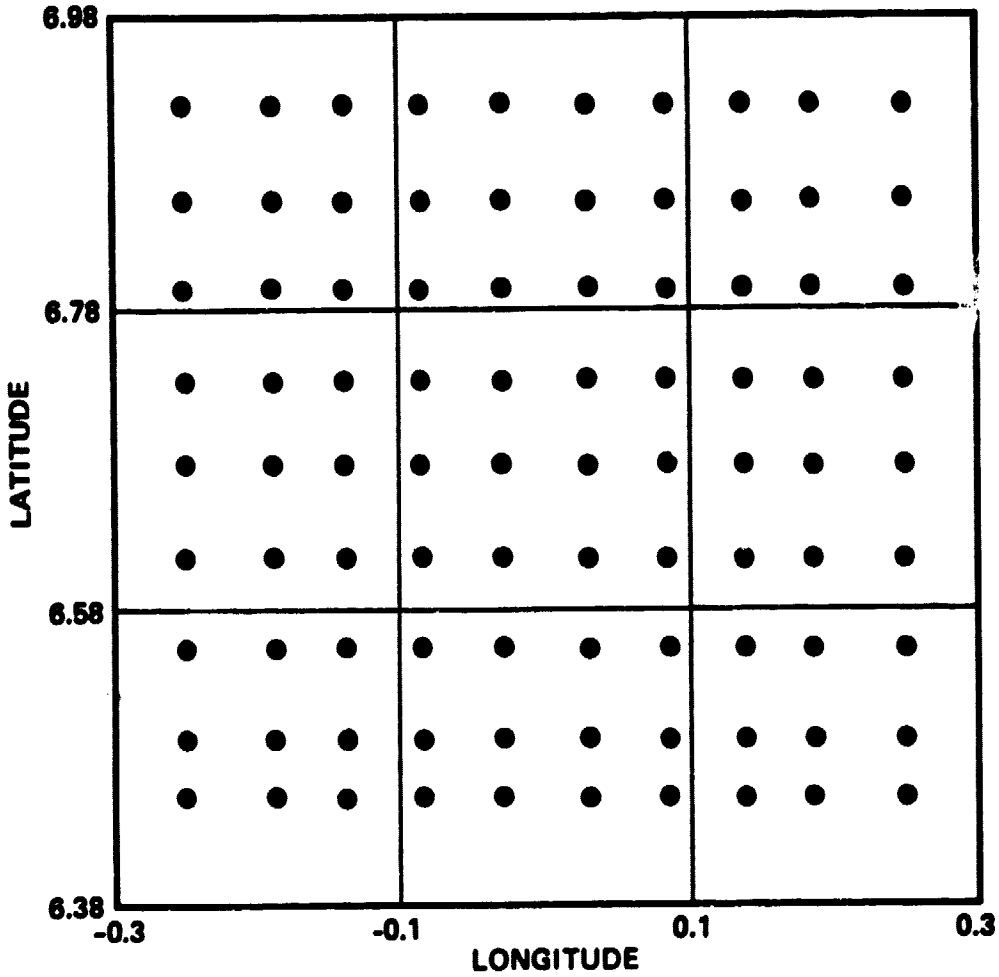

Figure 2. LAMMR Data Density Superimposed on a 20 km by 20 km Grid

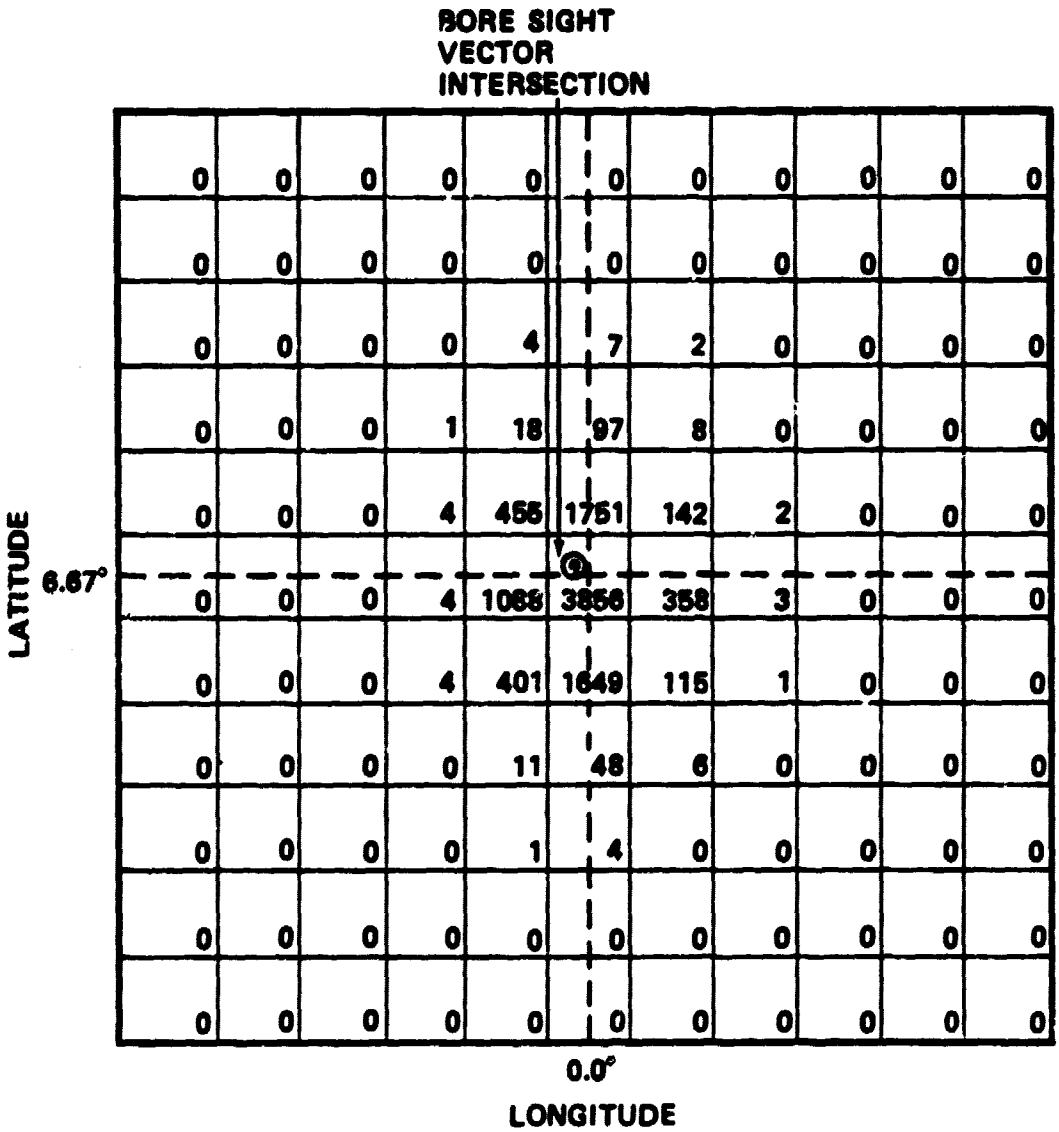

Figure 3. Fractional Response x 10^4 of an Antenna Observation (4.3 GHz) to a 20 km by 20 km Grid

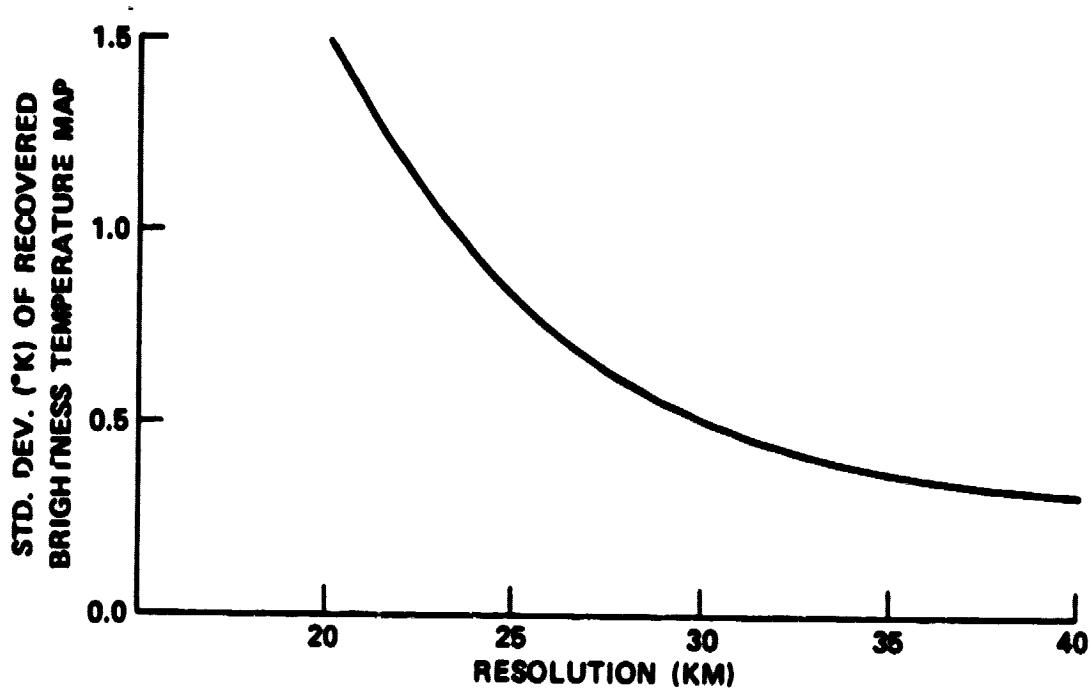

Figure 4. Standard Deviation of the Estimated Brightness Temperature Map as a Function of Resolution